sciendo

Civil and Environmental Engineering
Vol. 18, Issue 1, 280-291, DOI: 10.2478/cee-2022-0026

BENDING BEHAVIOR OF FIBERGLASS TEXTILE-REINFORCED THIN GEOPOLYMER MORTAR PANELS

Layth A. AL-JABERI[1,*], Zinah Waleed ABBAS[1], Osamah M. AL-KERTTANI[1], Mazin M. SARHAN[1]

[1] Civil Engineering Department, College of Engineering, Mustansiriyah University, Baghdad, Iraq.
[*] corresponding author: dr.laythal_jaberi@uomustansiriyah.edu.iq

Abstract

Textile-Reinforced Mortar (TRM) or Textile-Reinforced Concrete (TRC) can produce novel structural techniques in civil engineering fields. The current study experimentally investigated the bending behavior of thin geopolymer mortar panels reinforced with Fiberglass Textile Grids (FGTG). The experimental work totally consisted of twelve panel specimens divided into two groups; each group included six specimens. The first specimen of each group was unreinforced, whereas the rest of the specimens were reinforced with a different number of grids; however, each group's molarity of NaOH solutions was different. The results showed that the flexural strength and compressive strength of geopolymer mortar were significantly increased with the increment of molarity of NaOH solutions by 33 %. Textile reinforced geopolymer mortar (TRGM) panels showed deflection hardening behavior and multiple cracking. The deflection values at the same load levels were decreased when the number of grids and the molarity of NaOH solutions were increased. For TRGM specimens, in addition, the difference in molarities of NaOH solutions depicted a clear influence on the number and propagation of cracks. The toughness values of TRGM specimens were importantly enhanced with the increase of the FGTG reinforcement ratio.

Keywords:

Geopolymer;
FGTG grids;
Textile;
Bending;
Fly ash.

1 Introduction

Portland Cement (PC) concrete has been considered the most famous building material due to its properties and availability of its primary raw materials worldwide. The applications of PC effectively contributed to the development of modern civilizations and their economic growth. However, the production of PC has important limitations regarding the manufacturing process. Manufacturing of PC negatively affects the sustainability of the environment; high amounts of CO_2 are emitted because enormous energy and resources are required in the production process. Also, PC suffers from deterioration defects in harsh environments; then, a reduction in the safety of structural design can occur, negatively affecting the serviceability behavior of concrete members [1, 2].

Geopolymer cement has recently been investigated and used, manufacturing in a different process than the PC. Raw materials of Geopolymer Mortar (GPM) or Geopolymer Concrete (GPC) can be obtained by the kaolinite heat treatment or by materials products such as fly ash, clay, different silicon, and aluminium-containing industrial wastes. The production of geopolymer raw materials requires a low processing temperature leading to a reduction in energy consumption and CO_2 emissions in comparison with the production of PC [3, 4]. According to Davidovits (1994) [3], the geopolymer can be produced with a 60 % reduction in energy consumption and 80 - 90 % reduction in CO_2 emissions compared with the production process of PC; thus, geopolymer cement is a valuable option for environmental protection. Geopolymers can be made by combining alumino-silicate reactive materials and highly alkaline solutions, curing at room temperature.

GPM or GPC offer all three attributes necessary for outstanding construction and industrial applications because of their functional strength, stronger resistance to chemical attack, and higher

© Author(s) 2022. This work is distributed under the Creative Commons BY 4.0 license (https://creativecommons.org/licenses/by/4.0/).

temperature tolerance. These characteristics may be significant depending on the ultimate goal. However, workability, setting time, and long-term durability attributes such as minimum porosity and excellent efflorescence stability are still considered challenging topics for many researchers [3]. Numerous studies have shown that new building processes, like 3D printing, benefit from GPM or GPC's rheological qualities [4].

Clay and different silicon and aluminium-containing industrial wastes are utilized as raw materials in the production of geopolymers. Fly ash (FA), created during coal combustion, is frequently employed in construction to improve workability, stabilization, strength, and durability [5]. Also, FA is commonly used as a source of geopolymer concrete. The spherical particles in FA, which help establish pores in the binder, help reduce paste viscosity. Calcined kaolin clay or Metakaolin (MK) has the advantage of being chemically consistent and possessing good thermal reactivity and low permeability. Mixing water demand and yield stress are increased due to the high fineness of MK. Other effects include damage to the pore structure, lower durability, and higher efflorescence. More investigations have been done on each system's reactions, binders, and microstructure. Economic potential and excellent engineering properties are offered by using fly ash to replace metakaolin in re-designing mixtures [6, 7].

Composite materials have widely been used in construction projects using the characteristics of the materials together. For instance, the concrete is used to resist the compression loads in reinforced concrete members, whereas the reinforcement is used to resist the tension loads. Textile reinforced concrete (TRC) provides designers with opportunities to design thin-section concrete members having both high compressive and tensile strengths. The TRC is a relatively new material, where multiple fabric layers are employed with fine-grained concrete. TRC reinforcement has recently resulted in innovative cementitious composites having a significant strength and ductility under static and dynamic loading. TRC displays closer, narrower and regular-spread cracks in tension and flexural due to the alignment of the fiber [8].

Cracks in Fiber-Reinforced Concrete (FRC) are localized immediately upon occurrence, whereas fiber bridging promotes crack propagation throughout the specimen in TRC. Secondary cracks form due to the high energy required to extend existing cracks. Single-crack localization becomes diffused, resulting in macroscopic pseudo-strain hardening. Increased mechanical bond strength of textiles in the matrix results in structural hardening and various cracking behaviors. As shown in Fig. 1, the tension stiffening effect of the TRC system can be defined as the capacity of the uncracked segments in between the two parallel cracks to carry tensile force [9]. TRC can present 2 - 3 times higher strength and ductility than FRC [10].

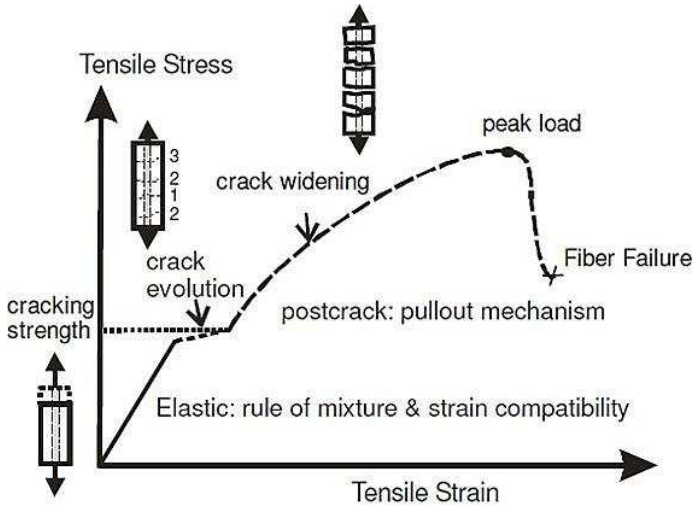


Fig. 1: Tensile response of a TRC system [9].

Strain hardening materials are resistant to fatigue and impact, making them excellent for usage in industrial buildings, highways, bridges, and locations prone to earthquakes, hurricanes, and severe wind stress [9]. On the other hand, concrete elements reinforced with TRC can be lighter, more flexible, and more slender than concrete elements reinforced with other types of reinforcement. TRC is suitable for numerous application areas, including lightweight concrete members, repairing or strengthening structural elements, and thin-walled structures [11-12]. However, because that TRC is

innovative material, additional researches are necessary to ensure the safety design of TRC reinforced concrete members [13].

In the current study, the flexural behavior of thin panels consisting of geopolymer mortar reinforced with textile grids were cast and tested under static bending. A total of twelve panel specimens were investigated and discussed. The load-deflection behavior, toughness, crack patterns of the tested panels were detailed and depicted. R.

2 Research significance

Only a few studies have been conducted on TRGM panels, such as Tamburini et al. [14], Shaikh et al. [15], Menna et al. [16], and Le Chi et al. [17]. According to these experiments, the textile grids transformed the matrix's brittleness to ductility and avoided stress localization in the first cark region. However, only a few numbers of the previous studies were carried out with FGTG grids; thus, there is a need to conduct more studies regarding this type of reinforcement under different conditions of manufacturing and loading. This research examines the behavior of thin panels made of Metakaolin-Fly Ash based geopolymer mortar (MK-FA-GPM) reinforced with different numbers of FGTG grids under flexural loading. Also, the effects of NaOH solution concentrations in terms of molarity on compressive strength, modulus of rupture of the MK-FA-GPM matrix, and flexural behavior of FGTG reinforced thin panels are aimed to be studied. This study reached a novel, closely spaced and continuous FGTG grids reinforcement. This arrangement matches the concept of Ferrocement, which is stated by (ACI CT-21: ACI Concrete Terminology) [18].

3 Experimental program

3.1 Materials of the geopolymer mortar

- The mortars' materials used in this study are shown as follows: (Metakaolin) (MK): They are clay mineral kaolinites having a de-hydroxylated form based on ASTM C618-19 [19]. The Kaolinites may lose most of their adsorbed water at a temperature range of 100 - 200 °C; furthermore, the de-hydroxylated forms can occur at 500 - 700 °C. The current study adopted an endothermic procedure to change the kaolinites to metakaolins; this conversion process requires tremendous energy to remove the hydroxyls chemically-bonded ions by destroying the crystal structure kaolinites, producing amorphous silica and alumina phases having notable surface areas. According to previous studies [8], the optimal activation temperatures can range from 550 - 850 °C; based on Snellings R. et al. (2012), the temperature range is 650 - 750 °C is considered the most likely to be used. The chemical components of MK are detailed in Table 1.
- Fly ash (FA) - Class F is replaced 0.25 % of MK weight. FA is compatible with ASTM C 618-19 [19]. The chemical components of FA-Class F are detailed in Table 1. The specific gravities and fineness of both MK and FA are listed in Table 2.

Table 1: Chemical components of MK and FA.

Compounds	SiO_2	Al_2O_3	Fe_2O_3	SO_3	MgO	CaO	K_2O	Na_2O	LOI
MK [%]	51.59	38.11	1.82	0.14	0.23	0.45	0.43	0.11	6.12
FA [%]	65.65	17.69	5.32	0.22	0.85	0.97	2.32	1.35	2.77

Table 2: Specific gravities and fineness of MK and FA.

Powder	Specific gravity	Fineness [m^2/kg]
MK	2.61	1100
FA	2.33	773

- Alkaline activators include NaOH solutions (8 and 12 molar concentrations) and Na2SiO3 solutions.
- Quartz sand: having a maximum size of 2.36 mm.
- Quartz powder: having a maximum size of 60 µm, approximately.
- Superplasticizer admixture for concrete: high range, according to ASTM C494 / C494M – 19 [20].

- Fiberglass Textile Grids (FGTG): commercial meshes having high-strength and alkali resistance roving fibers, the fiber rovings equally distributed in two orthogonal directions (0°/90°). More details regarding this FGTG woven mesh are presented in Table 3.

Table 3: Details of used textile.

Weight	160 g/m^2
Slot mesh	4 mm x 4 mm
Slot thickness	0.52 mm
Tensile strength	2000 N/mm^2

3.2 Mixing design and preparing procedure of the geopolymer mortar

Homogeneity and excellent bonding between the fibers and matrix within the composite are essential. Thus, the mortar design should include fine to very fine particles and high workability. These two conditions play an important role in the penetration process of mortar particles through holes of the FGTG. The high fineness of MK and FA (Table 2) and the inclusion of quartz powder can achieve the first condition. Spherical silt-sized particles of fly ash, water and superplasticizers ensure high workability. The mixed proportions of geopolymer mortars are detailed in Table 4.

Furthermore, blending the materials to produce the GPM matrix was essential for an appropriate mix. GPM prepared with a ratio of 1:1 of geopolymer-based materials (MK and FA) and alkaline activators. The NaOH solution was produced with the two concentrations of 8 Molar and 12 Molar by dissolving the high 98 % purity NaOH flakes in water. Then, the prepared NaOH solution was mixed with Na_2SiO_3 solution after 24 hours to get the alkaline solution activator Na_2SiO_3/NaOH; the mixing ratio of Na_2SiO_3/NaOH was 2.5. It is worth mentioning that Na_2SiO_3/NaOH was not used within the first 30 minutes of its production. The extra water demand of mortar and the superplasticizer dosage was found by flow diameter of 110 ± 5 mm. The preparation procedure of the GPM included three steps. Firstly, dry mixed base materials and sand were mixed for three minutes in the laboratory using a Hobart mixer. Secondly, the alkaline solution was mixed with extra water and the superplasticizer for five minutes. Finally, the liquid component was gradually added to the dry mix; it was done at a temperature of 23 ^oC.

Table 4: Mixed proportions of geopolymer mortars.

Metakaolin MK	Fly ash FA	Quartz sand > 0.6 mm	Quartz sand < 0.6 mm	Activator Na_2SiO_3 + NaOH	Water\(MK + FA)	SP by weight of MK + FA
0.75	0.25	2	0.2	1	0.28	0.02

3.3 Specimen details

The current study investigated twelve panel specimens having the dimensions of 450 mm x 450 mm x 20 mm tested under four-point bending. The specimens were divided into two groups (Group A and Group B); each consisted of six specimens reinforced with/without Fiberglass Textile Grids (FGTG) with different alkaline activators concentrations. The first specimen of each group was cast without reinforcement and considered the reference specimen, whereas the rest were reinforced with different numbers of layers of FGTG. Fig. 2 shows details of the tested panel specimens of the current study. Reinforcement details of Group A specimens were similar to those in Group B; however, the only difference between Group A and Group B was the NaOH concentrations used in the matrix composition. The NaOH concentrations were 8 Molar and 12 Molar for Group A and B, respectively. Table 5 presents details and configurations of the tested specimens. The panel specimens were labelled in three parts; the first part defines whether the specimen is to be reinforced or not; the second part represents the number of layers of FGTG reinforcement, and the third part represents the mortar type. Note that the reference specimens did not need to mention the number of layers of FGTG reinforcement.

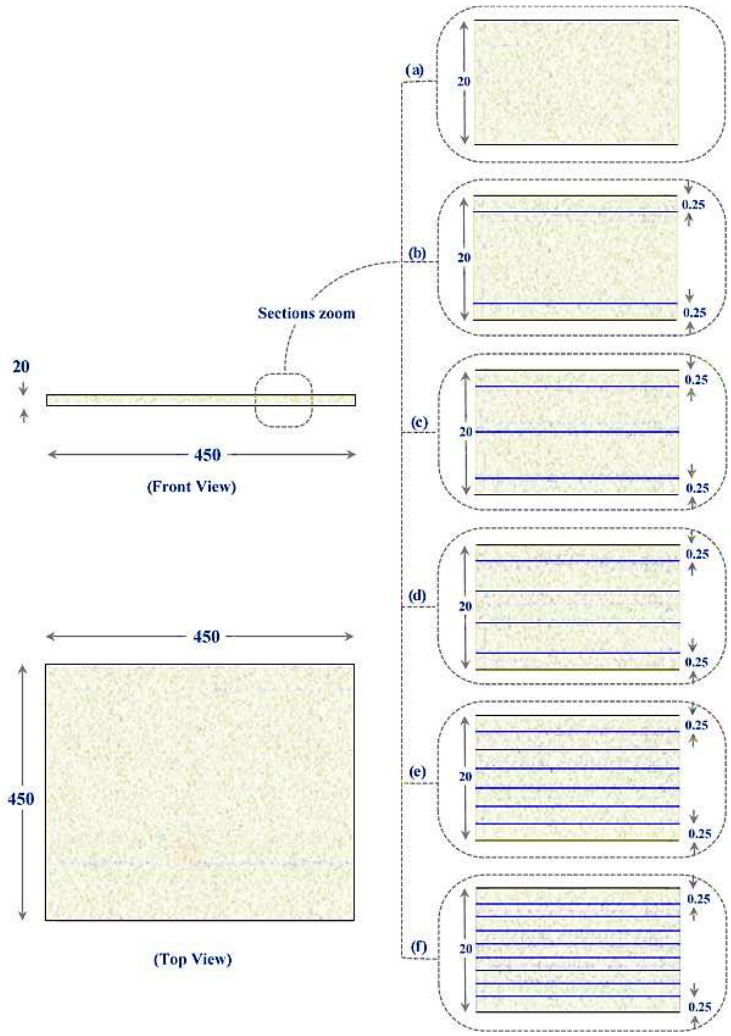


Fig. 2: Cross-section details of tested specimens-all dimensions in mm: a) Specimens GPM-8M & GPM-12M, b) Specimens TRGM 2-8M & TRGM 2-12M, c) Specimens TRGM 3-8M & TRGM 3-12M, d) Specimens TRGM 4-8M & TRGM 4-12M, e) Specimens TRGM 6-8M & TRGM 6-12M, and f) Specimens TRGM 8-8M & TRGM 8-12M.

Table 5: Details of specimens.

Group	Panel specimen	NaOH concentrations [Molar]	No. of layers of FGTG	Group	Panel specimen	NaOH concentrations [Molar]	No. of layers of FGTG
A	GPM-8M	8	0	B	GPM-12M	12	0
	TRGM 2-8M	8	2		TRGM 2-12M	12	2
	TRGM 3-8M	8	3		TRGM 3-12M	12	3
	TRGM 4-8M	8	4		TRGM 4-12M	12	4
	TRGM 6-8M	8	6		TRGM 6-12M	12	6
	TRGM 8-8M	8	8		TRGM 8-12M	12	8

3.4 Curing of specimens

After the casting process of specimens, the curing process was conducted for the casts. After wrapping the specimens in polypropylene film, they were cured for 1 day at room temperature. Each mix was sampled three times. Air curing for 28 days was followed.

3.5 Mechanical properties of geopolymer mortars

The mechanical properties of geopolymer mortars were obtained in terms of compressive strength and flexural strength according to BS EN 12390-3:2019 [21] and BS EN 12390-5:2019 [22]

respectively. The compressive strength of the geopolymer mortars was obtained based on the average of testing of three cubic samples having the dimensions of 50 mm x 50 mm x 50 mm. The flexural strength of the geopolymer mortars was obtained based on the average of testing of three prism samples having the dimensions of 160 mm x 40 mm x 40 mm.

3.6 Test setup of specimens

In both groups, all specimens were tested under four-point bending to depict their flexural behavior. A universal testing machine was used to achieve that purpose. A steel frame was particularly designed for the specimens' tests of this study. The steel frame consists of the loading arm and supporting frame; the loading arm consists of an IPE300 steel section. The support frame consists of four C100 welded together to obtain rigid support, steel rod of diameter 25 mm welded at the top of the frame to obtain a roller boundary condition. The load was applied slowly in increments of 0.5 kN until static failure. The load was statically applied using a slow increments rate of 0.5 kN. It reported the cracking load as the load at which the first crack was detected. In order to monitor the strain behavior of the specimens, strain gauges were used. The strain gauges were at the bottom mid-span of specimens where the maximum bending occurs. A multi-channel strain meter registered the strains. The test setup arrangement is shown in Fig. 3.

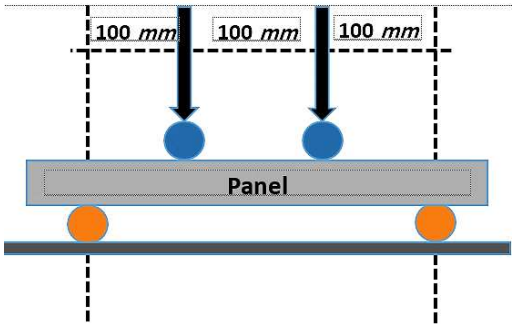


Fig. 3: Specimen arrangement under loading.

4 Results and discussion

4.1 Compressive strength and flexural strength of GPM

The compressive strength *Fcu* and flexural strength *Fr* of GPM were obtained after 28 days of the casting; their results are depicted in Fig. 4. It can be seen that the molarity of NaOH solution significantly affects the *Fcu* and *Fr* magnitudes of GPM; they increase when the molarity of NaOH solution increases. The compressive strength of GPM increased by 20 % when the molarity of NaOH solution increased up to 12M. Furthermore, the flexural strength of GPM increased by 29 % when the molarity of NaOH solution increased up to 12M. These increments were compatible with those reported in S. V Patankar (2014), in which the strength enhanced when the molarity of sodium hydroxide solution increased up to 13 M; additionally, higher Alkaline/FA ratios were introduced higher strength. However, the high molarity relatively decreased the workability of the mix because a more viscous mix was exhibited.

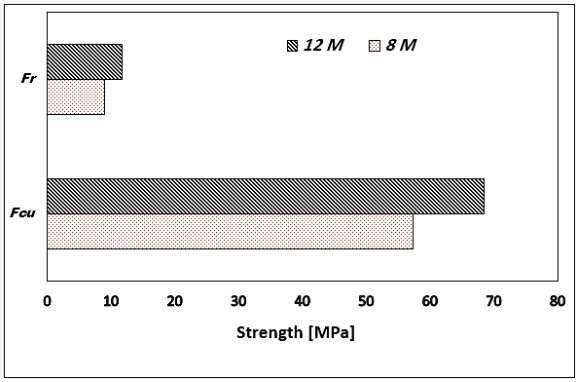


Fig. 4: Compressive strength *Fcu* and Flexural strength *Fr* of GPM (in [MPa] unit).

4.2 Load deflection relationships and toughness

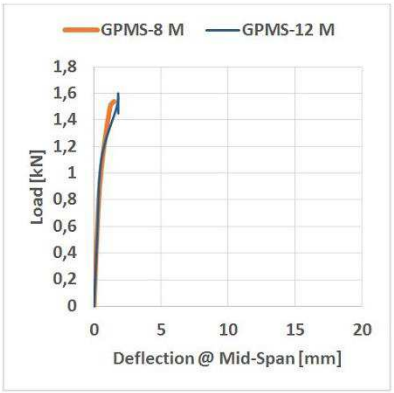
The load-deflection behaviour of panels was plotted; each figure represents a comparison between the different molarity of NaOH solutions, as shown in Fig. 5A-G. Fig. 5A showed that both of the panels conducted only an elastic behavior in spite of the difference in the molarity of NaOH solutions. This manner, compared with Fig. 5B-G, indicates that the (Textile) reinforcement play a considerable role in the ductile behavior of (TRGM) panels. The behavior in Fig. 5A occurred due to the propagations of cracks from the tension zone to the compression zone without any resistance, and then a brittle failure was recorded. This brittleness of geopolymer was compatible with previous studies, for instance: N. Ranjbar et al. (2015) and N. Ranjbar et al. (2020). It is also noted that the ultimate load of Specimens GPMS-8 M and GPMS-12 M - 0 were 1.54 kN and 1.60 kN, respectively; the magnitudes are approximately same. In other words, it can be said that the difference in molarity of NaOH solution has not a significant effect on unreinforced specimens. Based on Table 5, the reinforced panels failed at the ultimate loads of 2.60 - 10.40 MPa. It can be noticed that the ultimate loads of reinforced panels were gradually enhanced while the deflection was slightly increased. Also derived from Fig. 5B-F, it is clearly seen that the reinforced panels conduct a hardening behavior, and no softening manner was observed. Moreover, this behavior had a styled manner depending on the reinforcement ratio. NaOH molarity had a clear impact on the results of TRGM specimens. Specimens that were cast with (12) molar of NaOH, showed better outcomes. Higher molarity may have enhanced the bonding strength between the textile and the matrix, contributing to the hardening behavior.

Fig. 5G provides the possibility to compare the load-deflection curves for all panels. This figure shows the significant difference in the performance of the panels under flexural loading based on the number of reinforcing layers and the properties of the mortar.

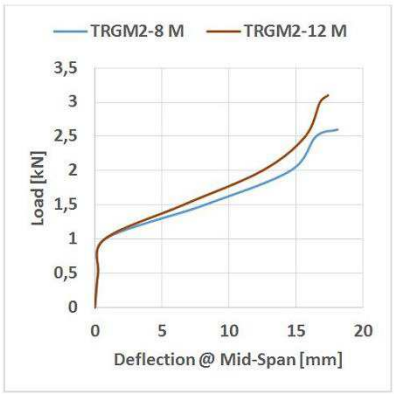
The Toughness of panels (UT) were computed and listed in Table 5; it was calculated as the area under the load-deflection curve of a specimen. Steadily increasing values of (UT) confirm more bearing ability in conjunction with the increase in the number of reinforcing layers and the improvement of the matrix. Energy absorption increased, and the specimens showed lower deflection at the same load levels, as shown in Fig. 6.

Table 5: Results of tested panels.

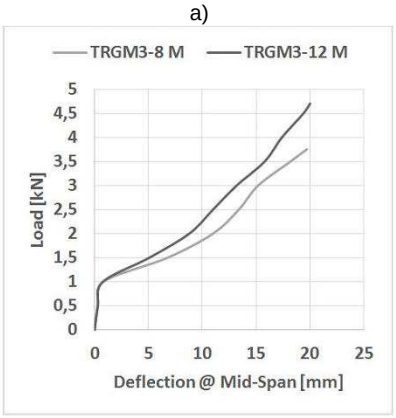
Specimen ID	First-crack load *Pcr* [kN]	Variance of *Pcr* [%]	Ultimate load *Pu* [kN]	Variance of *Pu* [%]	Ultimate deflection at mid-span [mm]	Toughness UT [kNmm]
GPMS-8 M	0.75	-	1.54	-	1.50	1.56
TRGM2-8 M	1.10	46.67	2.60	68.83	18.10	29.31
TRGM3-8 M	1.30	73.33	3.75	143.51	19.70	40.83
TRGM4-8 M	1.75	133.33	5.70	270.13	19.80	58.43
TRGM6-8 M	2.00	166.67	7.20	367.53	20.80	85.30
TRGM8-8 M	2.25	200.00	9.60	523.38	22.20	118.63
GPMS-12 M	0.80	-	1.60	-	1.80	1.98
TRGM2-12 M	1.25	56.25	3.10	93.75	17.40	30.15
TRGM3-12 M	2.00	150.00	4.70	193.75	20.00	49.03
TRGM4-12 M	2.25	181.25	6.20	287.50	20.30	68.88
TRGM6-12 M	2.50	212.50	8.20	412.50	21.40	98.04
TRGM8-12 M	2.75	243.75	10.40	550.00	21.50	122.39



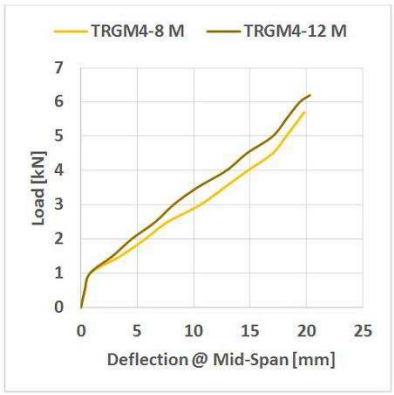
a)



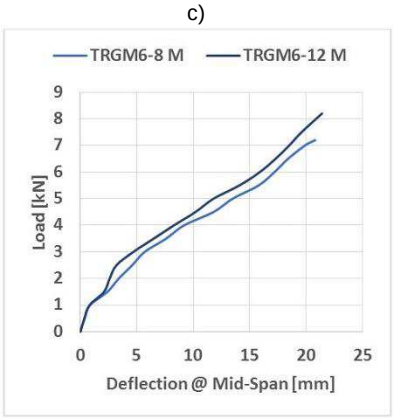
b)



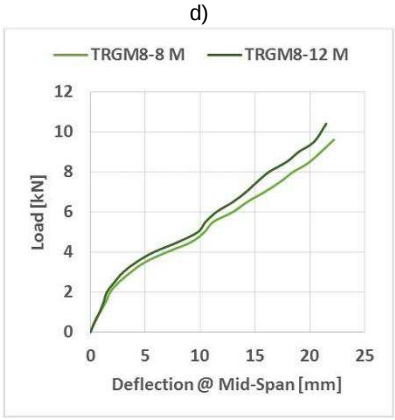
c)



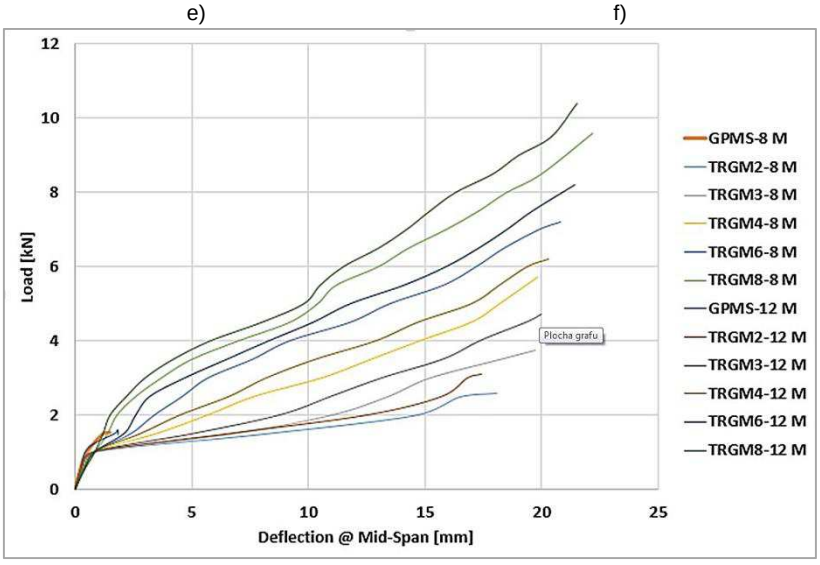
d)



e)



f)



g)

Fig. 5: Load-deflection curves of tested panels.

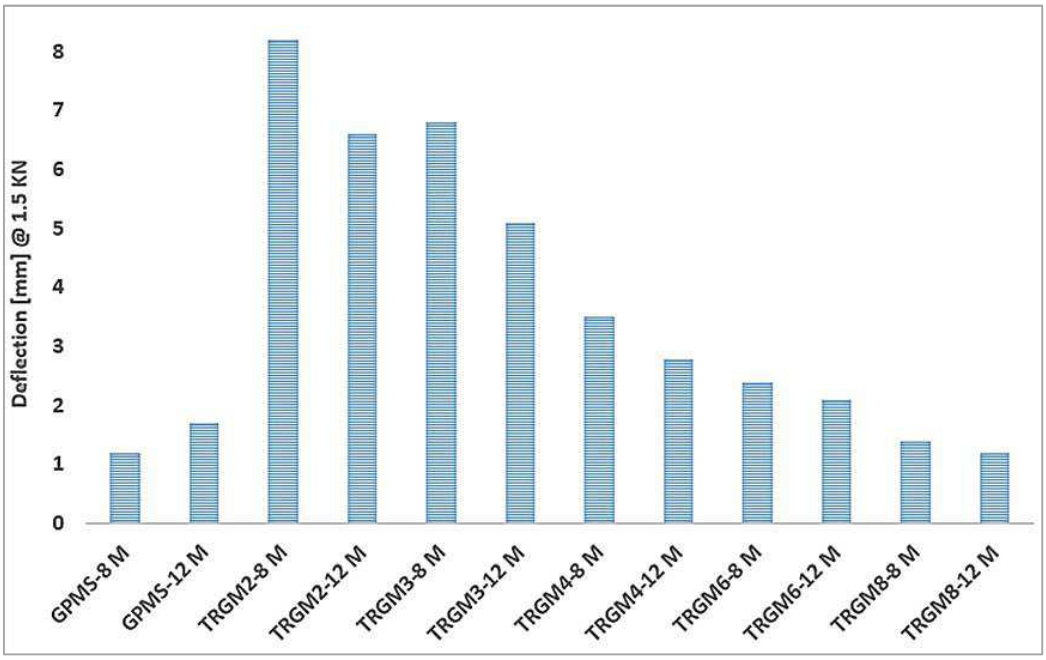


Fig. 6: Deflection [mm] at 1.5 kN.

4.3 Cracks pattern

The cracks patterns of reinforced panels were depicted in Fig. 7a-j. It can obviously be seen that the reinforcement ratio had an important effect on the cracks propagations in which the number of cracks increases with increase of the reinforcement ratio. In Fig. 7a and b, it was observed a single main crack; this is because of the low reinforcement ratio of the specimens, and the stresses did not conduct a uniform distribution in the tension zone of specimens. This attitude is a tension strain-softening, while the load-deflection curves of these two specimens. According to Naaman and Reinhardt [23], the tension strain-softening material can be deflection-hardening or deflection-softening.

In Fig. 7c and d, it was observed that the cracks number of specimens a little bit increased in comparison with specimens of Fig. 7a and b. However, there was a remarkable difference in cracks number of specimens of Fig. 7c and d even though both of the specimens have the same reinforcement details; here, the molarity of NaOH solutions showed a significant effect on the structural behavior of (TRGM) specimens. For Fig. 7e-g, the behavior of cracks patterns were similar for the previous specimens in which the cracks number increased with increase of reinforcement ratio; but they were worthy to confirm that the molarity of NaOH solutions have the control over the number and pattern of cracks. It was stated that deflection-hardening behavior can be attributed to the better matrix properties and good bonding between the fibers and matrix in addition to the number of textiles [16, 24].

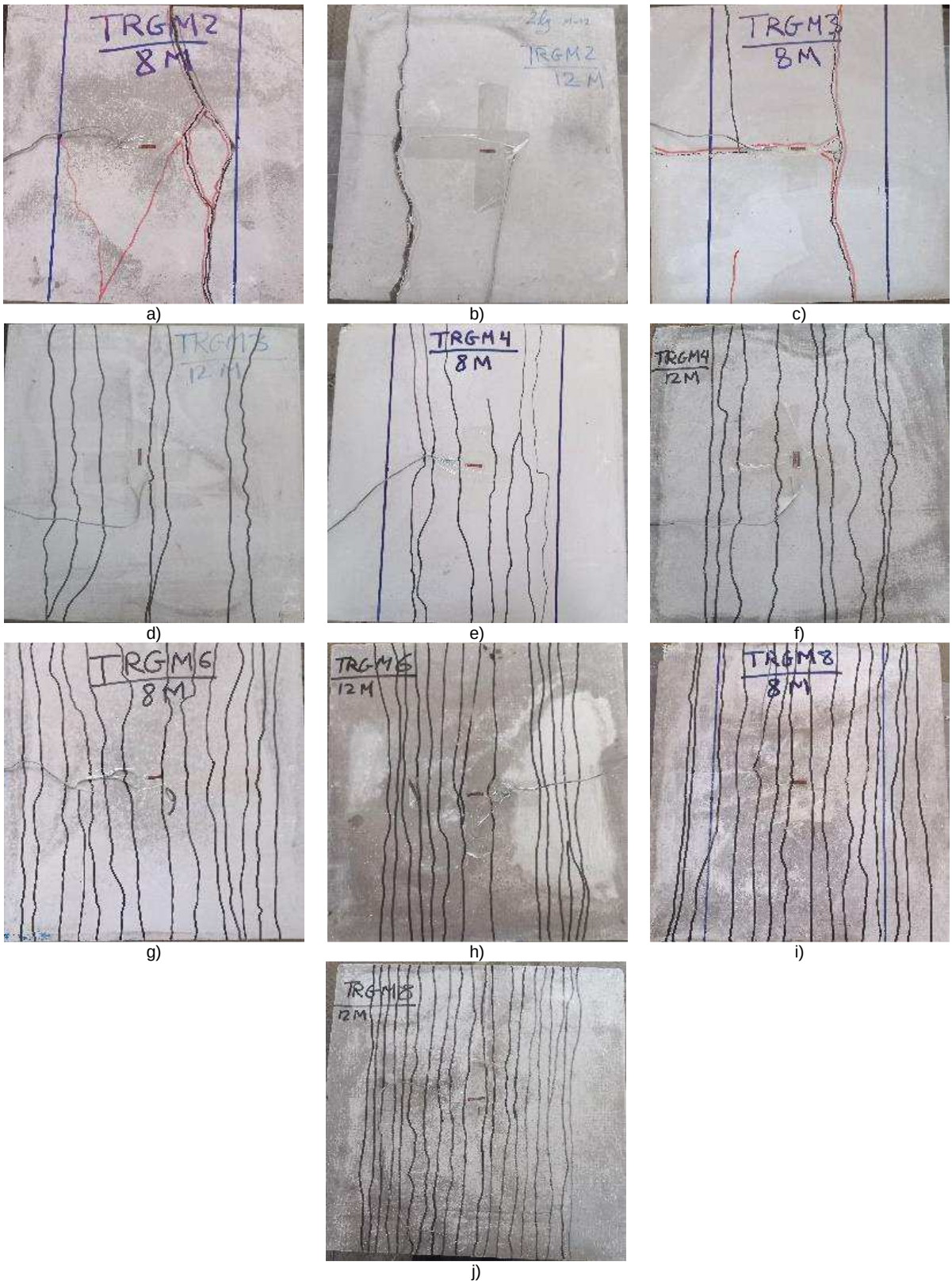


Fig. 7: The crack pattern of tested panels.

5 Conclusions

1) The compressive strength and flexural strength of geopolymer were significantly increased when the molarity of NaOH soultuion increased up to 12M

2) The (TRGM) specimens distinctly conducted a hardening behavior and no softening behavior was observed.

3) The unreinforced specimens exhibited brittle behavior with sudden failure regardless the molarity of NaOH solutions ratio.

4) For specimens casted with the NaOH solution of 8 M, the ultimate load of the specimens reinforced with two mesh layers, three mesh layers, four mesh layers, six mesh layers, and eight mesh layers increased by 68.83 %, 143.51 %, 270.13 %, 367.53 %, and 523.38 %, respectively compared with the unreinforced specimen.

5) For specimens casted with the solution of 12 M, the ultimate load of the specimens reinforced with two mesh layers, three mesh layers, four mesh layers, six mesh layers, and 8 mesh layers increased by 93.75 %, 193.75 %, 287.50 %, 412.50 %, and 550 %, respectively compared with the unreinforced specimen

6) The toughness of TRGM specimens were importantly enhanced with the increase of reinforcement ratio.

7) For unreinforced specimens, the difference in molarities of NaOH solutions showed approximately no effect on the ultimate loads and the deflection failure.

8) For reinforced specimens, the difference in molarities of NaOH solutions showed a clear effect on the number and propagation of cracks.

9) For specimens poured with the solution of 8 M, the first crack load of the specimens reinforced with two mesh layers, three mesh layers, four mesh layers, six mesh layers, and eight mesh layers improved by 46.67 %, 73.33 %, 133.33 %, 166.67 %, and 200 %, respectively, compared with the unreinforced specimen.

10) For specimens poured with the solution of 12 M, the first crack load of the specimens reinforced with two mesh layers, three mesh layers, four mesh layers, six mesh layers, and eight mesh layers improved by 56.25 %, 150 %, 181.25 %, 212.50 %, and 243.75 %, respectively, compared with the unreinforced specimen.

11) Due to increased textile layers and a better matrix, the panels exhibit decreasing deflection values at the same load levels.

Acknowledgements

The authors wish to acknowledge the Faculty of Engineering, Al-Mustansiriyah University, Baghdad, Iraq (www.uomustansiriyah.edu.iq), for their support in the present work.

References

[1] IGHALO, J. O. – ADENIYI, A. G.: A perspective on environmental sustainability in the cement industry. Waste Disposal & Sustainable Energy, 23. 2 (2020), pp. 161-164, https://doi.org/10.1007/S42768-020-00043-Y.

[2] PACHECO-TORGAL, F. – LABRINCHA, J. A. – LEONELLI, C. – PALOMO, A. – CHINDAPRASIRT, P.: Handbook of Alkali-Activated Cements, Mortars and Concretes. Elsevier Inc., 2014, https://doi.org/10.1016/C2013-0-16511-7.

[3] DAVIDOVITS, J.: Properties of Geopolymer Cements. First international conference on alkaline cements and concretes, Institute on Binders and Materials, Kiev, 1994, pp. 1-19.

[4] XIA, M. – SANJAYAN, J. G.: Methods of enhancing strength of geopolymer produced from powder-based 3D printing process. Materials Letters, 227, 2018, pp. 281-283.

[5] CHINDAPRASIRT, P. – KAMPALA, A. – DAPROM, P. – JITSANGIAM, P. – HORPIBULSUK, S.: Role of Fly Ash on Strength Properties of Rejuvenated Soil Cement for Pavement Materials. Civil and Environmental Engineering, Vol. 17, Iss. 2, 2021, pp. 583-596, https://doi.org/10.2478/cee-2021-0059.

[6] SARASWATHY, R. – JAMES, J. – PANDIAN, P. K. – SRIRAM, G. - SUNDAR, J. K. – KUMAR, G. S. - KUMAR A. S.: Valorization of Crushed Glass as a Potential Replacement for Sand in Cement Stabilized Fly Ash Bricks. Civil and Environmental Engineering, Vo. 15, Iss. 1, 2019, pp. 48-57, https://doi.org/10.2478/cee-2019-0008.

[7] ZHANG, P. – WANG, K. – WANG, J. – GUO, J. – LING, Y.: Macroscopic and microscopic analyses on mechanical performance of metakaolin/fly ash based geopolymer mortar. Journal of Cleaner Production, Vol. 294, 2021, pp. 126-193, https://doi.org/10.1016/J.JCLEPRO.2021.126193.

[8] HANEIN, T. – THIENEL, K. C. – ZUNINO, F. et al.: Clay calcination technology: state-of-the-art review by the RILEM TC 282-CCL. Materials and Structures, Vol. 55, Iss. 3, 2022, https://doi.org/10.1617/s11527-021-01807-6.

[9] MOBASHER, B.: Development of Design Procedures for Flexural Applications of Textile Composite Systems Based on Tension Stiffening Models. 6th Colloquium on Textile Reinforced Structures (CTRS6), 2011.
[10] SORANAKOM, C. – MOBASHER, B.: Flexural analysis and design of textile reinforced concrete. 4th Colloquium on Textile Reinforced Structures, CTRS4, 2009.
[11] BRAMESHUBER, W.: RILEM TC 201-TRC: Textile reinforced concrete- state-of-the-art. Vol. 36, RILEM publications, 2006.
[12] KOUTAS, L. N. – TETTA, Z. – BOURNAS, D. A. - TRIANTAFILLOU, T. C.: Strengthening of concrete structures with textile reinforced mortars: state-of-the-art review. Journal of Composites for Construction, Vol. 23, Iss. 1, 2019, 3118001.
[13] MOBASHER, B.: Mechanics of fiber and textile reinforced cement composites, 1st Editio, CRC press, London, 2011, https://doi.org/10.1201/9781315119151.
[14] TAMBURINI, S. – NATALI, M. – GARBIN, E. – PANIZZA, M. – FAVARO, M. – VALLUZZI, M. R.: Geopolymer matrix for fiber reinforced composites aimed at strengthening masonry structures. Construction and Building Materials, 141, 2017, pp. 542-552, https://doi.org/10.1016/J.CON BUILDMAT. 2017.03.017.
[15] SHAIKH, F. – HAQUE, S.: Behaviour of Carbon and Basalt Fibers Reinforced Fly Ash Geopolymer at Elevated Temperatures. International Journal of Concrete Structures and Materials, Vol. 12, Iss. 1, 2018, pp. 1-12, https://doi.org/10.1186/s40069-018-0267-2.
[16] MENNA, C. – ASPRONE, D. – FERONE, C. – COLANGELO, F. – BALSAMO, A. – PROTA, A. – CIOFFI, R. – MANFREDI, G.: Use of geopolymers for composite external reinforcement of RC members. Composites Part B: Engineering, Vol. 45, Iss.1, 2013, pp. 1667-1676, https://doi.org/ 10.1016/J.COMPO SITESB.2012.09.019.
[17] LE CHI, H. – LOUDA, P. - LE VAN, S. – VOLESKY, L. – KOVACIC, V. – BAKALOVA, T.: Composite Performance Evaluation of Basalt Textile-Reinforced Geopolymer Mortar. Fibers, Vol.7, Iss. 7, 2019, p. 63, https://doi.org/10.3390/fib7070063.
[18] ACI (American Concrete Institute), 2021. ACI Concrete Terminology. ACI CT-21. Farmington Hills, MI, ACI.
[19] ASTM C618 - 19, Standard Specification for Coal Fly Ash and Raw or Calcined Natural Pozzolan for Use in Concrete, ASTM International, West Conshohocken, PA, 2019, https://www.astm. org/Standards/C618.htm.
[20] ASTM C494 / C494M - 19, Standard Specification for Chemical Admixtures for Concrete, ASTM International, West Conshohocken, PA, 2019, https://www.astm.org/Standards/C494.
[21] BS EN 12390-3:2019, Testing hardened concrete-Part 3: Compressive strength of test specimens, 2019.
[22] BS EN 12390-5:2019 Testing hardened concrete Flexural strength of test specimens, 2019.
[23] NAAMAN ANTOINE, E. - REINHARDT HANS WOLF.: Proposed classification of HPFRC composites based on their tensile response. Materials and structures, Vol. 39, Iss. 5, 2006, pp. 547-555.
[24] DU, Y. – ZHANG, X. – ZHOU, F. – ZHU, D. – ZHANG, M. – PAN, W.: Flexural behavior of basalt textile-reinforced concrete. Construction and Building Materials, Vol. 183, 2018, pp. 7-21.